Performance Evaluation of Object-based and Pixel-based Building Detection Algorithms from Very High Spatial Resolution Imagery

Article *in* Photogrammetric Engineering and Remote Sensing · June 2014

DOI: 10.14358/PERS.80.6.519

CITATIONS
12

READS
420

3 authors:

Iman Khosravi
University of Tehran
19 PUBLICATIONS **84** CITATIONS
SEE PROFILE

Mehdi Momeni
University of Isfahan
26 PUBLICATIONS **145** CITATIONS
SEE PROFILE

Maryam Rahnemoonfar
University of Maryland, Baltimore County
58 PUBLICATIONS **436** CITATIONS
SEE PROFILE

Performance Evaluation of Object-based and Pixel-based Building Detection Algorithms from Very High Spatial Resolution Imagery

Iman Khosravi, Mehdi Momeni, and Maryam Rahnemoonfar

Abstract

This paper reviews and evaluates four building extraction algorithms including two pixel-based and two object-based methods using a diverse set of very high spatial resolution imagery. The applied images are chosen from different places (the cities of Isfahan, Tehran, and Ankara) and different sensors (QuickBird and GeoEye-1), which are diverse in terms of building shape, size, color, height, alignment, brightness, and density. The results indicate that the performance and the reliability of two object-based algorithms are better than pixel-based algorithms; about 10 percent to 15 percent better for the building detection rate and 6 percent to 10 percent better for the reliability rate. However, in some cases, the detection rate of pixel-based algorithms has been greater than 80 percent, which is a satisfactory result. On the other hand, segmentation errors can cause limitations and errors in the object-based algorithms, so that the commission error of object-based algorithms has been higher than pixel-based algorithms in some cases.

Introduction

Building detection from very high spatial resolution (VHSR) imagery has been an active research topic over the past few years. Up to now, several building detection algorithms have been proposed in the literature which can be divided into two categories: pixel-based methods and object-based methods. In the first group, only pixels and often their spectral attributes are used (Hester *et al.,* 2008). On the other hand, the processing unit of the second group is an object, where the non-spectral attributes of the objects (such as proximity and geometry attributes) can be used in addition to their spectral attributes (Chubey *et al.*, 2006).

A strategy of some building detection methods in the first category uses only the clustering methods (Wei *et al.*, 2004). The combination of clustering and segmentation methods is used in some papers (e.g., Hai-yue *et al.*, 2006; Jiang *et al.*, 2008; Ghanea *et al.*, 2011). There are some pixel-based methods which use the combination of spectral and morphological indices such as differential morphology profile (DMP) or the morphological attribute profiles (APs) (Jin and Davis, 2005; Mura *et al.*, 2010; Huang and Zhang, 2011; Huang and Zhang, 2012). Some papers have used only morphological methods (Meng *et al.*, 2009). Another strategy of some pixel-based methods is the combination of spectral indices, clustering and morphological methods (Aytekin *et al.*, 2012).

In the second category (object-based methods), the most important step is segmentation (Blaschke, 2010). Benz *et al.* (2004) and Taubenbock *et al.* (2010), presented an object-based, multi-level hierarchical classification method based on a multi-resolution segmentation to detect the urban features. Bouziani *et al.* (2010) detected building by a rule-based classification method based on an automatic region growing segmentation. More recently, an edge-based segmentation has been used in some papers (e.g., Kanjir *et al.*, 2008; Hu and Weng, 2011) to classify urban features especially building regions. Meng *et al.* (2012) presented a hybrid approach of object-based and morphology-based methods to detect residential buildings from lidar data and aerial images. In a recent paper, a classifier ensemble strategy based on combining pixel-based and object-based processing is presented to detect urban features (Huang and Zhang, 2013).

Up to now, a few papers have compared the pixel-based and object-based analysis for classifying urban features especially buildings (Wang *et al.*, 2007; Cleve *et al.*, 2008; Myint *et al.*, 2011). Therefore, the present study aims to compare pixel-based and object-based analysis for detecting building. For this purpose, four building detection algorithms are reviewed which the first two algorithms are pixel-based and similar to the works proposed by Ghanea *et al.* (2011) and Aytekin *et al.* (2012) and the rest of the algorithms are object-based approaches performed by *eCognition® Developer* and *ENVI Feature Extraction* software. This paper has tried to use a diverse set of VHSR images for comparing these algorithms. The applied images are chosen from different places and two different sensors, i.e., QuickBird and GeoEye-1; they are diverse in terms of building shape, size, color, height, alignment, brightness, and density.

The reminder of paper is organized as follows: In the next Section, the data applied to this paper is explained, followed by the four aforementioned algorithms. Then, the result of each algorithm applied on the dataset and comparison between their performances is presented, followed by our conclusions.

Iman Khosravi and Mehdi Momeni are with the Department of Surveying Engineering, Faculty of Engineering, University of Isfahan, Isfahan, I.R. Iran (iman.khosravi@mihanmail.ir).

Maryam Rahnemoonfar is with the School of Engineering & Computing Sciences, Texas A&M University-Corpus Christi, TX.

Photogrammetric Engineering & Remote Sensing
Vol. 80, No. 5, June 2014, pp. 519–528.
0099-1112/14/8006–519

doi: 10.14358/PERS.80.6.519

Study Area and Test Data

Ten regions which are chosen from different places and different sensors are shown in Figure 1a to 1j (in the form of gray images); regions (a), (e), (f), (g), (i), and (j) are the pan-sharpened QuickBird images (0.6 m resolution), and region (h) is the pan-sharpened GeoEye-1 image (0.5 m resolution at stereo mode) of the City of Isfahan. Region (d) is the pan-sharpened GeoEye-1 image (at nadir mode) of the City of Tehran, and regions (b) and (c) are the pan-sharpened QuickBird images of the City of Ankara. All the images are preprocessed by histogram stretching to enhance. There are many different urban objects such as roads, yards, shadows, vegetation, green spaces, bare land, and the most important feature, i.e. buildings, in these images. The images can be considered as a diverse set of VHSR images in terms of "building alignment and distance, density, shape, size, color, and reflectance, the presence of shadow and vegetation, variation of buildings height and imaging angle."

Based on the most prominent property of each region, the ten regions in Figure 1 are categorized as follows: regions (a) and (b) have the buildings with regular alignment where the former has blocks of buildings while the latter has single buildings. Region (c) has the buildings with irregular alignment. The building density of region (d) is relatively high. Moreover, its buildings have different shape and size. The troublesome urban objects, i.e., shadow and vegetation areas can be observed in proximities of buildings in regions (g) and (h), respectively. The buildings of region (i) are variety in terms of height. The image of region (j) is an oblique image unlike the other regions. Finally, there is similar reflectance (or low contrast) between building and non-building areas in regions (k) and (l) where the former has blocks of buildings while the latter has single buildings. In addition, there is diversity in building color in all the regions except regions (b) and (c) (belonging to the City of Ankara).

Applied Building Detection Algorithms

A brief description of four building detection algorithms is given in this section. The first two pixel-based algorithms are similar to the work of Ghanea *et al.* (2011) and Aytekin *et al.* (2012) where the former is the combination of clustering and segmentation methods (*CS*) while the latter is the combination of spectral indices, clustering and morphological methods (*SCM*). The two other algorithms are object-based classification and the former uses an edge-based segmentation (*OB-ES*) and the latter multi-resolution segmentation (*OB-MS*).

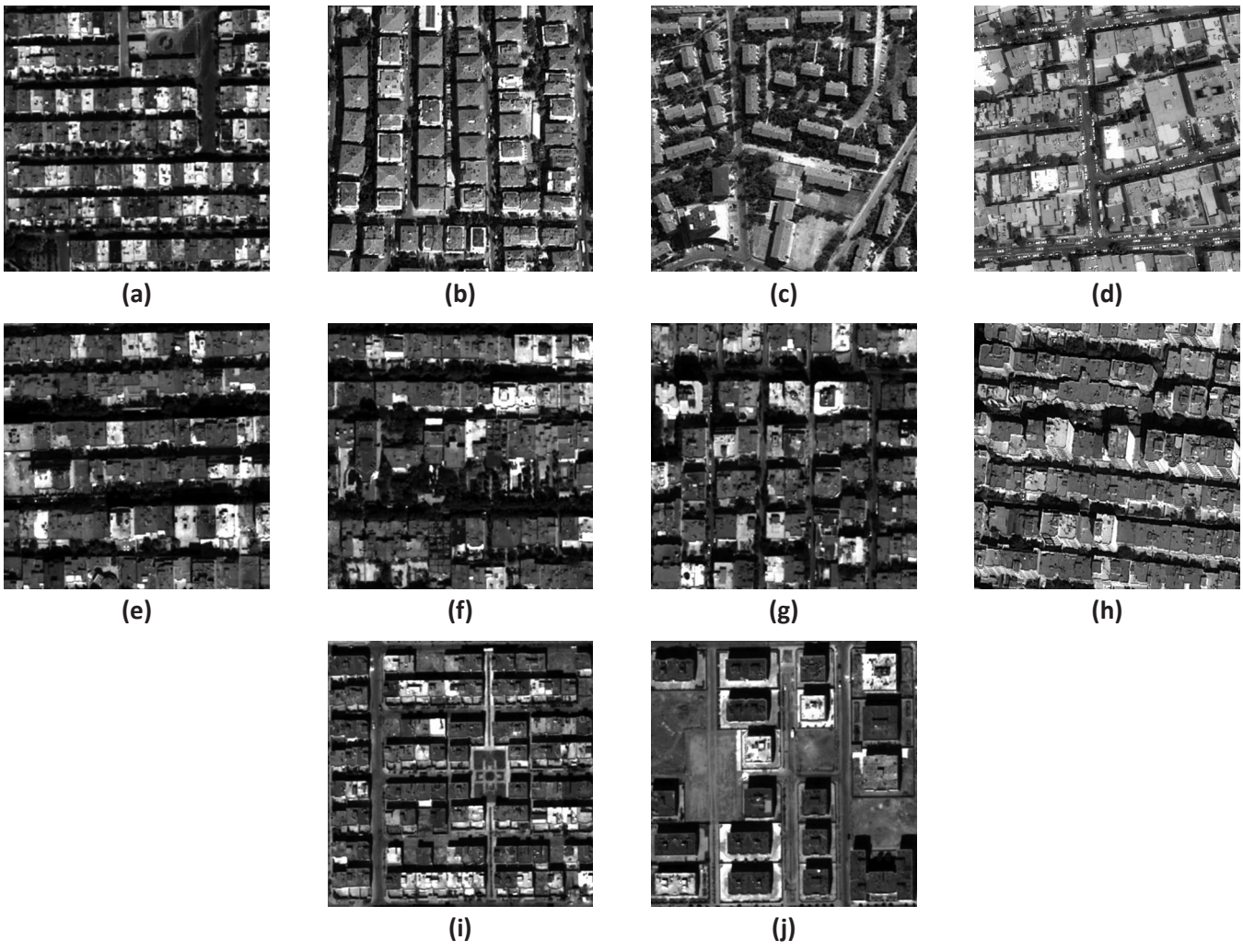

Figure 1. A diverse set of VHSR images applied in this paper (in the form of gray images): (a) Regular alignment and building blocks, (b) Regular alignment and single buildings, (c) Irregular alignment, (d) Positional dense, (e) Troublesome shadows, (f) Troublesome vegetation, (g) Variation of height (h) Oblique image, (i) Similar reflectance and building blocks, and (j) Similar reflectance and single buildings.

Pixel-based Algorithms

Algorithm CS (Clustering and Segmentation)
Algorithm *CS* presented by Ghanea *et al.* (2011) includes these steps: in the first step, a k-means clustering (K = 2) is applied to the original image to convert it to a binary image. This image consists of the semi-building layer and the non-building layer. Then, a closing morphological operator is used to cover the small non-building areas surrounded by the semi-building layer. Afterwards, a fuzzy c-means (FCM) clustering is applied to the semi-building layer to split it into several clusters. Each cluster is decomposed into independent areas using the connected component labeling process. After FCM clustering, the algorithm applies two approaches to remove pseudo-building areas (some remaining bare lands and roads). In the first approach, the small pseudo-building areas are removed using an area thresholding. The area of the smallest building is considered as the value for this threshold. In the second approach, a region-growing segmentation is applied to remove the large pseudo-building areas. The variance and the area of the segments are used as the similarity criterion for segmenting. The value of threshold for area is the area of the largest building. In addition, the variance of all points belonging to each segment at the previous step is considered as the variance threshold for that segment. Finally, the holes of the segments are removed using a filling morphological operator, and in this way, only the building areas are detected. Figures 2a to 2f show the procedure of *CS* algorithm.

Algorithm SCM (Spectral indices, Clustering and Morphological)
Algorithm *SCM* was presented by Aytekin *et al.* (2012) and has these steps: in Step 1, the images of the vegetation index (NDVI) and the shadow index (the ratio of chromaticity to intensity in YIQ color space) are produced. Then, a suitable threshold is determined based on Otsu's method for each them to remove the vegetation and shadow areas. After masking out the vegetation and shadow areas, the basic image is segmented using a mean-shift method. Thus, man-made areas (include mainly the building rooftops and roads) can be extracted after the classification of the vegetation and shadow areas. Afterwards, a modified version of the thinning algorithm (Aytekin *et al.*, 2012) is applied to each segment and then the main roads are separated from other segments using Otsu's thresholding. Next, the small artifacts are filtered using the principle component analysis (PCA) and a morphological operator (bwareaopen). Finally, only building areas are remained in the image. The procedure of *SCM* algorithm is shown in Figure 3a to 3f.

Object-based Algorithms

Algorithm OB-ES (Object-Based Classification by Edge-Based Segmentation)
Algorithm *OB-ES* detected buildings using the object-oriented framework of *ENVI Feature Extraction* software. In the first step, an edge-based segmentation algorithm is applied to the image. This algorithm requires two parameters for segmenting

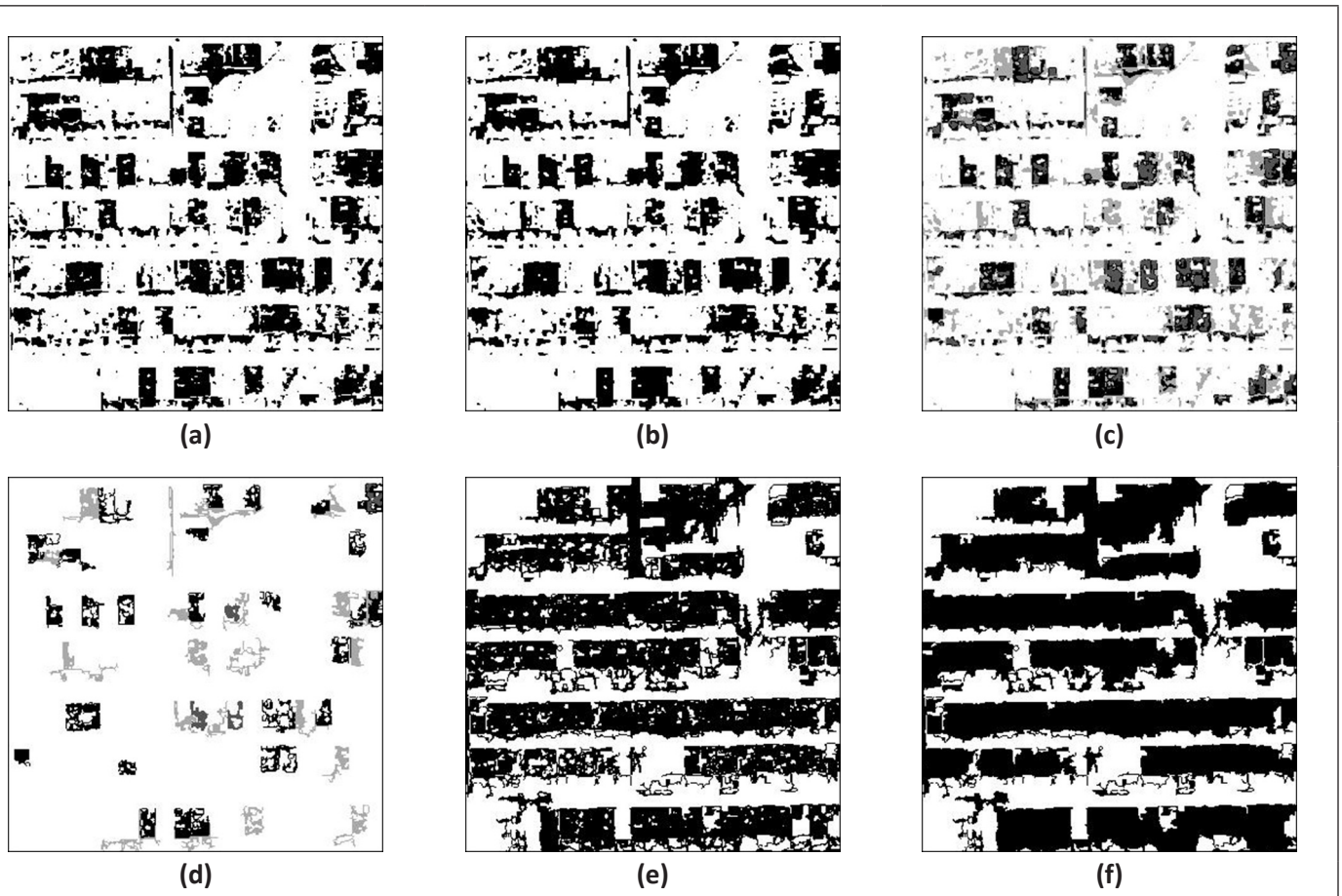

Figure 2. The procedure of *CS* algorithm: (a) Binary image using k-means clustering with k = 2 (semi-building layer is white and non-building layer is black), (b) Post-processing using closing morphological operator, (c) Image clustering using FCM, (d) Removing the small pseudo-building regions using area thresholding, (e) Region-growing algorithm, and (f) Filling the holes and the final result of building detection.

image: scale and merge parameters (Holbling and Neubert, 2008). Then, the required spectral and non-spectral attributes are computed for all segments. One of the capabilities of *ENVI Feature Extraction* is the automatic selection of optimum attributes for classification (Holbling and Neubert, 2008). Next, all segments are labeled using either the K-nearest neighbor or the support vector machine classifier. Finally, the buildings are detected from the classified image. Figure 4a to 4d show the procedure of this algorithm.

Algorithm OB-MS (Object-Based Classification by Multi-resolution Segmentation)

Algorithm *OB-MS* has similar steps to the previous algorithm. However, this algorithm uses a multiresolution segmentation belonging to *eCognition® Developer* software (Chubey *et al.*, 2006). This algorithm requires three parameters: scale, shape, and compactness parameters (Baatz and Schape, 2000). After producing segments, classes such as roads, vegetation, shadow, bare land and buildings are defined. Then, mean values for NDVI, green and brightness, area, length to width ratio, rectangular fit, and shape index are selected as object attributes. Finally, *OB-MS* algorithm determines the label of each segment using a nearest neighbor classifier based on fuzzy logic and then, the buildings are detected from the classified image. The procedure of *OB-MS* algorithm is shown in Figure 5a to 5c.

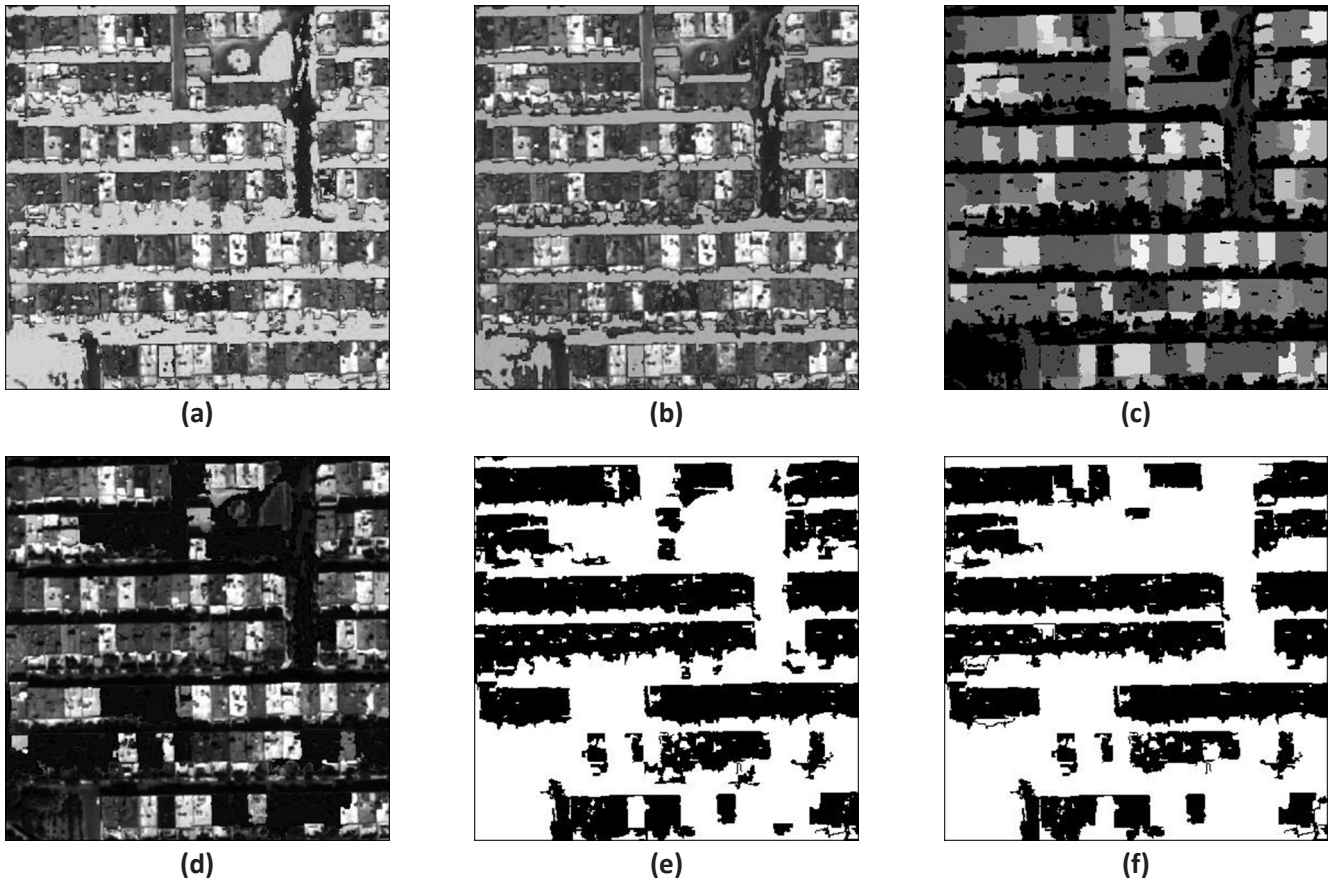

Figure 3. The procedure of *SCM* algorithm: (a) Masking vegetation (gray areas show masked vegetation), (b) Masking shadows (gray areas show masked shadows), (c) Man-made image (non-black areas show man-made regions), (d) Masking roads (black areas show masked roads), (e) Filtering the artifacts using PCA and bwareaopen operator, and (f) The final resulting image of building detection.

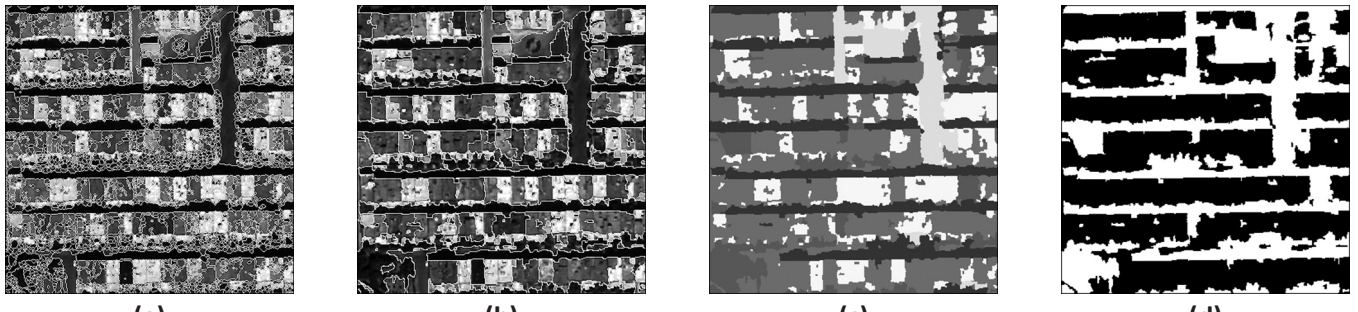

Figure 4. The procedure of *OB-EC* algorithm: (a) Image segmentation_scale level, (b) Image segmentation_merging level, (c) Classified image, and (d) The final resulting image of building detection.

Implementation and Evaluation Results

Four algorithms are applied to ten regions and are compared together in this section. For example, Figure 6a to 6d show the detected buildings images of regions (b), (c), and (h) according to all of the algorithms. In general, as shown in Figure 6, the detected buildings of object-based algorithms (Figure 6d and 6e) are more accurate and meaningful than pixel-based algorithms (Figures 6b and 6c). This may be due to the use of objects (or groups of pixels) instead of single pixels in the object-based algorithms.

The existing digital map of each region is considered as the reference date in this paper (Figure 6a). Then, the detected buildings by the four aforementioned algorithms are compared with the reference data, pixel by pixel. For evaluation, the common metrics used in most building detection studies are employed such as building detection rate (DR), false negative rate (FNR), reliability (R), false positive rate (FPR), and overall accuracy (OA). The metrics are defined as follows (Khoshelham *et al.*, 2010):

$$DR = \frac{TP}{TP + FN} \tag{1}$$

$$FNR = \frac{FN}{TP + FN} \tag{2}$$

$$R = \frac{TP}{TP + FP} \tag{3}$$

$$FPR = \frac{FP}{TN + FP} \tag{4}$$

$$OA = \frac{TP + TN}{TP + FN + FP + FN} \tag{5}$$

In Equations 1 to 5, *TP* refers to the pixels detected correctly as buildings; *FP* refers to the falsely detected buildings; *FN* refers to the pixels, which could not be detected as buildings although they exist in the reference data; and finally *TN* refers

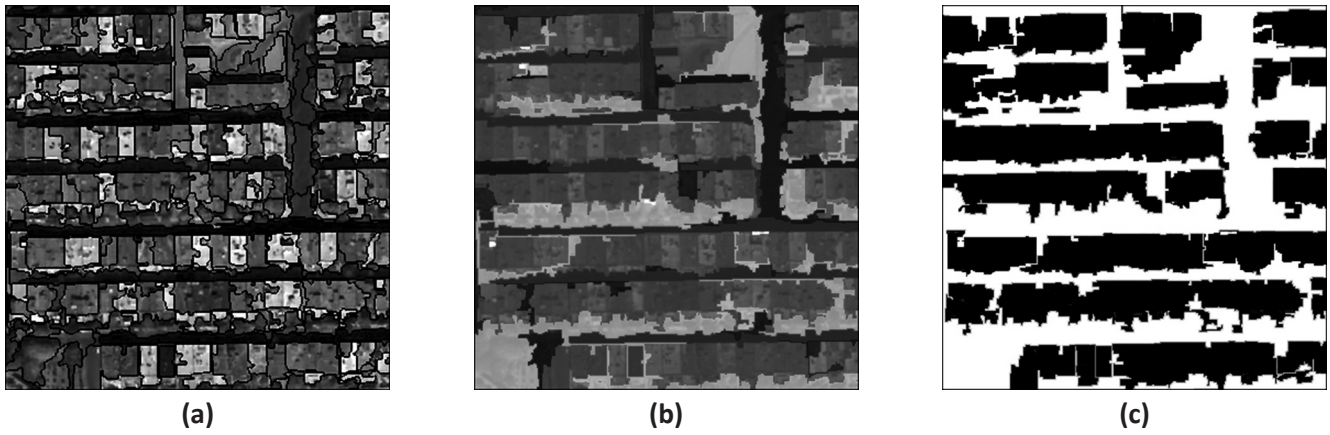

Figure 5. The procedure of *OB-MS* algorithm: (a) Multiresolution segmentation, (b) Classified image, and (c) The final resulting image of building detection.

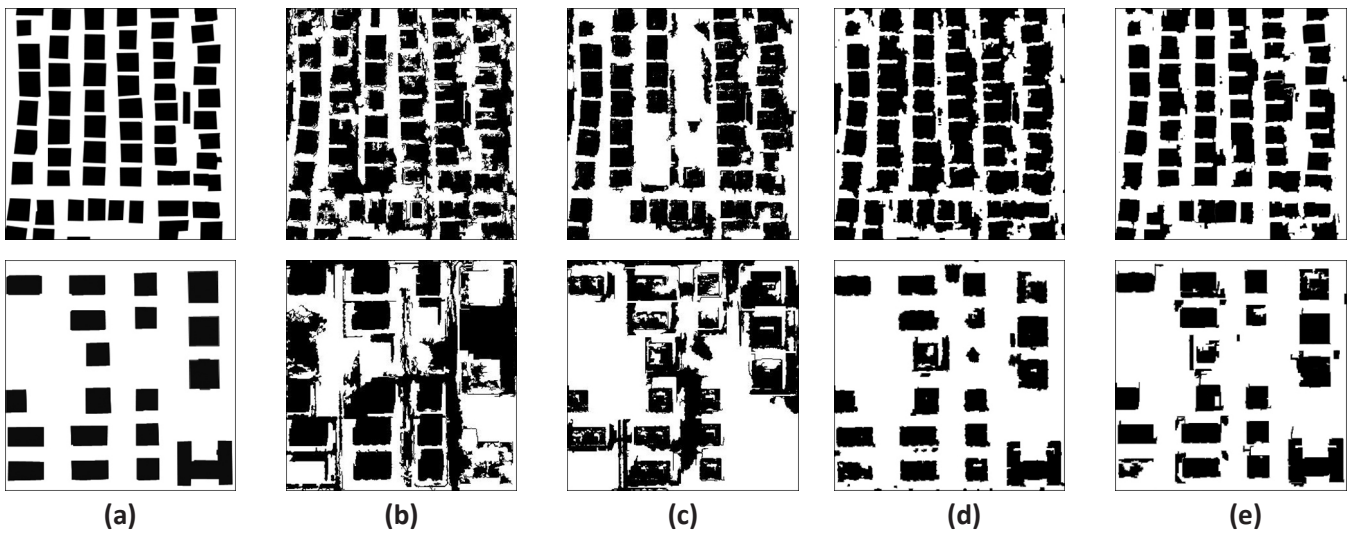

Figure 6. The resulting building images of four algorithms: (a) Reference date; the existing digital map of regions (b) and (j). The buildings image of (b) *CS* algorithm (pixel-based), (c) *SCM* algorithm (pixel-based), (d) *OB-ES* algorithm (object-based), and (e) *OB-MS* algorithm (object-based).

to the pixels detected correctly as non-buildings (Lee *et al.*, 2003). A higher DR value with a lower FNR value indicates the better performance of an algorithm in the building detection, and a high *R* and a low *FPR* imply the reliability of the results.

The Results of Pixel-based Algorithms (Algorithms CS and SCM)

Tables 1 and 2 show the evaluation results of building detection from *CS* and *SCM* algorithms (pixel-based), respectively. According to the tables, the DR value of these two algorithms is between around 40 percent (41 percent) to 89 percent. In addition, the R value of *CS* and *SCM* algorithms differs from 34 percent to 81 percent and 47 percent to 84 percent, respectively. It is noteworthy that the minimum DR (or maximum omission error (FNR)) of two algorithms belongs to region (i) in Figure 1 with around 40 percent (about 60 percent FNR), where there is similar reflectance between building *blocks* and non-building areas (Figure 7b and 7c). In addition, the R of the two algorithms at region (j) in Figure 1 is the lowest (with around 34 percent and 47 percent, respectively) i.e., where there is similar reflectance between *single* buildings and non-building areas. Moreover, the maximum commission error (FPR) of *CS* algorithm belongs to this region (with about 46 percent). For *SCM* algorithm, it belongs to region (h) in Figure 1 with 32 percent, where the imaging angle is oblique (Figure 8b and 8d).

The average DR of the two algorithms for all regions is about 77 percent and 72 percent. Moreover, the average R of them is about 65 percent and 72 percent. In detail, *CS* algorithms at regions (a) through (f) and (h) in Figure 1 and *SCM* algorithm at regions (e) through (h) in Figure 1 have a DR greater than 80 percent. Another conclusion can be drawn from tables is that the DR values of *CS* algorithm are more stable than *SCM* algorithm due to the lower standard deviation of the DR of it (14.6 versus 15.1). Conversely, the R values of *SCM* algorithm are more stable than *CS* algorithm (with 13 versus 17 of STD).

The average FNR of the two algorithms is about 23 percent and 28 percent and the average FPR of the two algorithms is about 29 percent and 22 percent. As shown in Figures 9a and 9b, the omission error (FNR) of *CS* algorithm is lower than *SCM* algorithm at all regions except regions (e), (g), and (i) in Figure 1, while the commission error (FPR) of *SCM* algorithm is lower than *CS* algorithm at all regions except region (g). In addition, the stability of FNR values of *CS* algorithm is more than *SCM* algorithm, whereas the FPR values of *SCM* algorithm are more stable than *CS* algorithm.

The Results of Object-based Algorithms (Algorithms OB-ES and OB-MS)

The evaluation results of building detection from two object-based algorithms (*OB-ES* and *OB-MS*) are presented in Tables 3 and 4. According to the tables, the DR values of *OB-ES* algorithm is between 77 percent and 95 percent (average 87 percent), and it is between 73 percent and 95 percent (average 86 percent) for *OB-MS* algorithm. These values show the higher performance of object-based algorithms than pixel-based algorithms. Moreover, comparing the average R values of two object-based algorithms (79 percent to 78 percent) with two pixel-based algorithms (65 percent to 72 percent) indicates that the results of object-based algorithms are more reliable than pixel-based algorithms.

According to Tables 3 and 4, the stability of *OB-MS* algorithm is higher than *OB-ES* algorithm at R, FPR, and OA values due to the lower standard deviation, while the DR and FNR values of *OB-ES* algorithm are more stable than *OB-MS* algorithm. The OA value of *OB-ES* algorithm is between 73 percent and 95 percent (average 83 percent), and that of *OB-MS* algorithm is between 76 percent and 91 percent (average 83 percent). These values are around 7 percent to 9 percent higher than pixel-based algorithms (74 percent and 76 percent).

TABLE 1. ACCURACY ASSESSMENT RESULTS OF CS ALGORITHM (%)

Region	DR	R	FNR	FPR	OA
Region (a)	81.53	75.00	18.47	28.17	76.77
Region (b)	81.28	71.30	18.72	26.90	76.79
Region (c)	86.87	44.26	13.13	31.38	72.69
Region (d)	79.84	69.09	20.16	25.23	76.87
Region (e)	88.69	81.20	11.31	25.37	81.40
Region (f)	89.38	79.85	10.62	21.75	83.71
Region (g)	74.54	75.44	25.46	25.95	74.30
Region (h)	82.72	74.61	17.28	36.60	74.32
Region (i)	40.05	50.25	59.95	25.62	60.90
Region (j)	67.86	33.56	32.14	45.69	57.75
MINIMUM	40.05	33.56	10.62	21.75	57.75
MAXIMUM	89.38	81.20	59.95	45.69	83.71
AVERAGE	77.28	65.46	22.72	29.27	73.55
STD	14.61	16.58	14.61	7.05	8.22

TABLE 2. ACCURACY ASSESSMENT RESULTS OF SCM ALGORITHM (%)

Region	DR	R	FNR	FPR	OA
Region (a)	66.56	84.80	33.44	12.36	76.91
Region (b)	74.14	73.22	25.86	22.29	76.10
Region (c)	67.44	58.74	32.56	27.81	70.93
Region (d)	57.50	73.31	42.50	14.90	70.39
Region (e)	88.98	83.83	11.02	21.77	84.24
Region (f)	87.34	82.79	12.66	17.59	84.83
Region (g)	84.82	76.72	15.18	27.53	78.86
Region (h)	81.32	76.84	18.68	31.89	75.58
Region (i)	40.62	59.24	59.38	18.06	65.72
Region (j)	66.50	47.05	33.50	25.77	72.24
MINIMUM	40.62	47.05	11.02	12.36	65.72
MAXIMUM	88.98	84.80	59.38	31.89	84.83
AVERAGE	71.52	71.65	28.48	22.00	75.58
STD	15.10	12.60	15.10	6.28	6.06

Comparison between Algorithms

The most important difference between the object-based algorithms (*OB-ES* and *OB-MS* algorithms) and the pixel-based algorithms (*CS* and *SCM* algorithms) can be observed in the results of regions (i) and (j) in Figure 1, where there is similar reflectance between building and non-building areas. From tables, the DR (FNR) values of object-based algorithms are approximately 20 percent to 40 percent higher (lower) than the one of pixel-based algorithms for these two regions (refer to Figure 9a). The reason could be due to the use of segments or objects instead of single pixels and also non-spectral attributes (e.g., spatial and geometry attributes) in the object-based process.

In addition, as noted earlier, the results of pixel-based algorithms in region (j) in Figure 1 have the lowest reliability compared to the other regions, whereas the R values of object-based algorithms are 40 percent to 60 percent more than the one of pixel-based algorithms. Moreover, the FPR values of object-based algorithms at this region are the lowest (4 percent and 7 percent i.e., 20 percent to 40 percent lower). However, the commission error of object-based algorithms has been (about 3 percent to 11 percent) more than pixel-based algorithms for

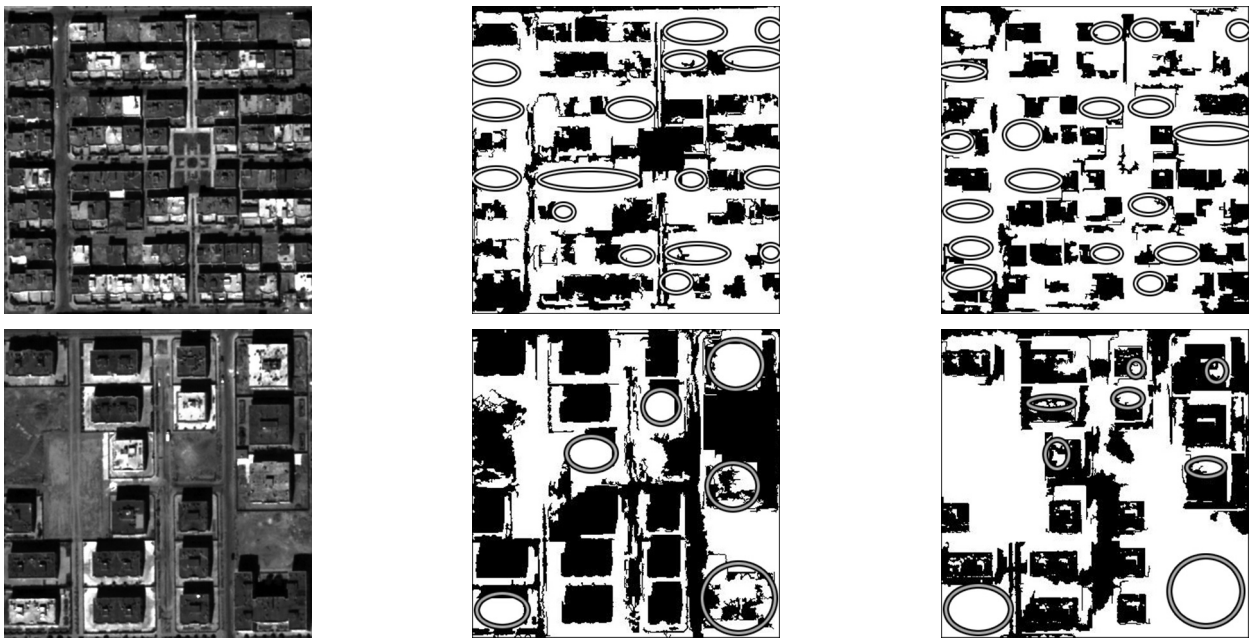

Figure 7. (a) Regions (i) and (j), (b) The building detection result of *CS* algorithm, and (c) The building detection result of *SCM* algorithm (The ellipses show the omission error).

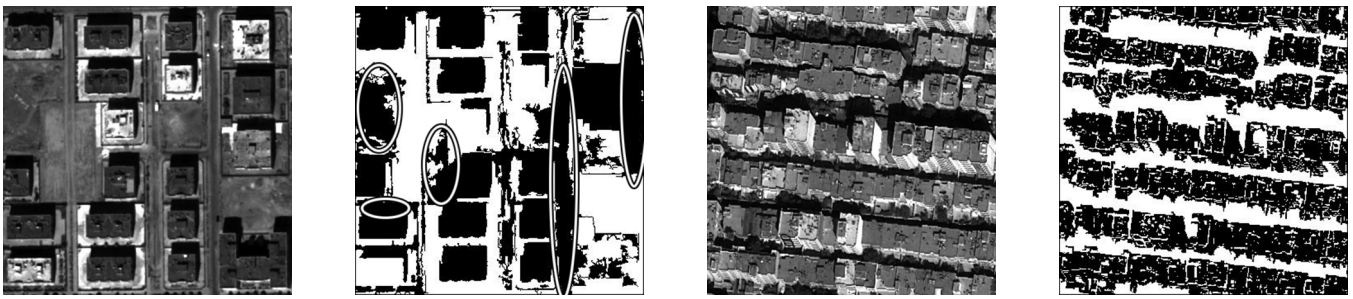

Figure 8. The maximal commission error of pixel-based algorithms: (a) Region (i), (b) The building detection result of *CS* algorithm, (c) Region (h), and (d) The building detection result of *SCM* algorithm.

region (i), where there is similar reflectance between building blocks and non-building areas (refer to Figure 9b).

However, at some cases, the DR value of pixel-based algorithms was higher than object-based algorithms. For example, the DR value of *CS* algorithm is more than *OB-ES* algorithm at region (e) and it is more than *OB-MS* algorithm at region (h). In addition, the one of *SCM* algorithm is more than *OB-ES* algorithm at regions (e) and (g), and it is more than *OB-MS* algorithm at regions (g) and (h). In fact, the performance of the two pixel-based algorithms has been (around 3 percent) more than *OB-ES* algorithm at region (e), where there are shadow areas in proximities of buildings (Figure 10) and has been (around 10 percent) more than *OB-MS* algorithm at region (h), where there is the imaging angle is oblique (Figure 11).

In addition, the reliability rate of pixel-based algorithms was better than object-based algorithms. For example, the R values of *CS* algorithm has been more than *OB-ES* algorithm at regions (a), (d), and (f), and it is more than *OB-MS* algorithm at regions (d) and (f). The one of *SCM* algorithm has been more than *OB-ES* algorithm at regions (a), (d), (e), (f), and (h), and it is more than *OB-MS* algorithm at regions (a), (d), (e), (f), and (g).

On the other hand, object-based algorithms have produced higher commission error (FPR) than pixel-based algorithms for some regions (refer to Figure 9b). For example, *OB-ES* algorithm has a higher FPR compared to *CS* algorithm at regions (a), (d), (f), (h), and (i) and compared to *SCM* algorithm at regions (a), (b), (d), (f), (h), and (i). In addition, the FPR of *OB-MS* algorithm is more as compared to *CS* algorithm at regions (d), (f), (g), and (i), and it is more than *SCM* algorithm at regions (a), (d), (e), (f), (g), and (i). An example of this case is shown in Figure 12. One the main reasons for a higher omission or commission errors in object-based algorithms in comparison with pixel-based algorithms can be due to the over or under-segmentation errors. Therefore, it can be concluded that segmentation is both an advantage and a disadvantage for object-based analysis.

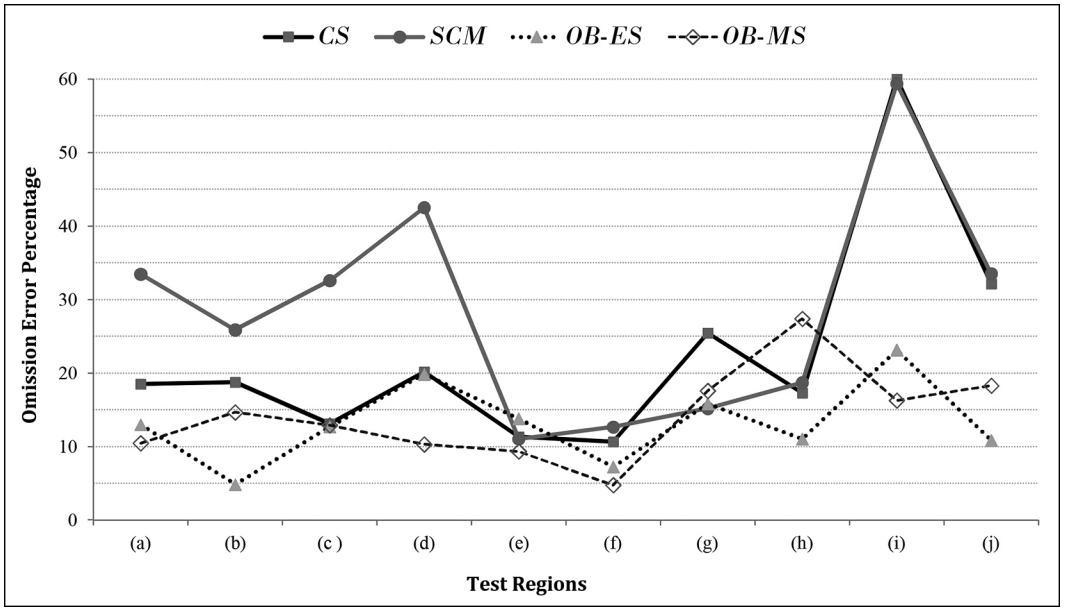

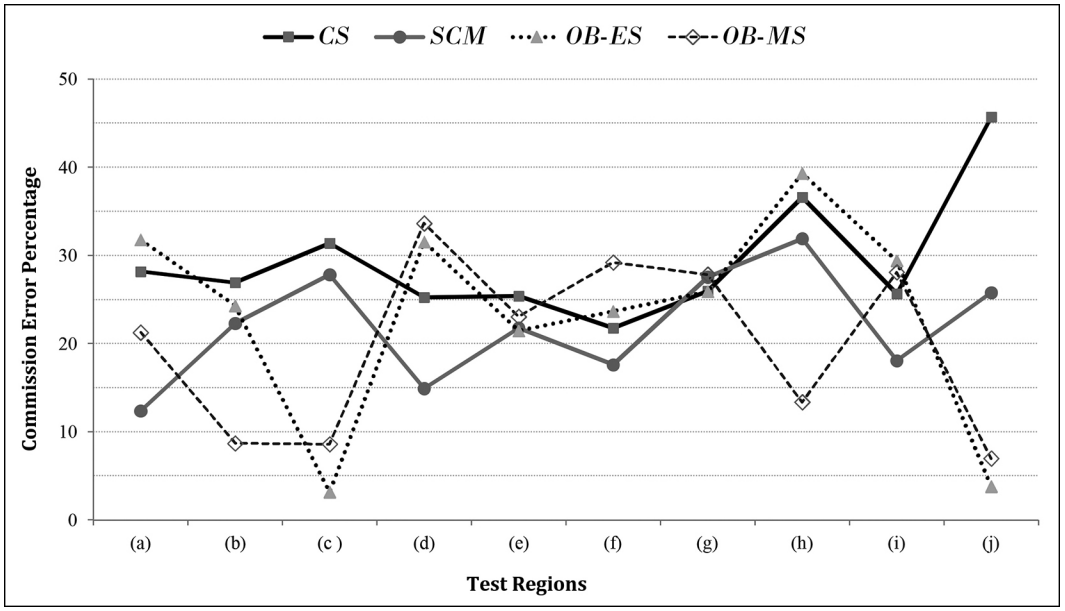

Figure 9. (a) Omission error (FNR) plot of four algorithms, and (b) Commission error (FPR) plot of four algorithms.

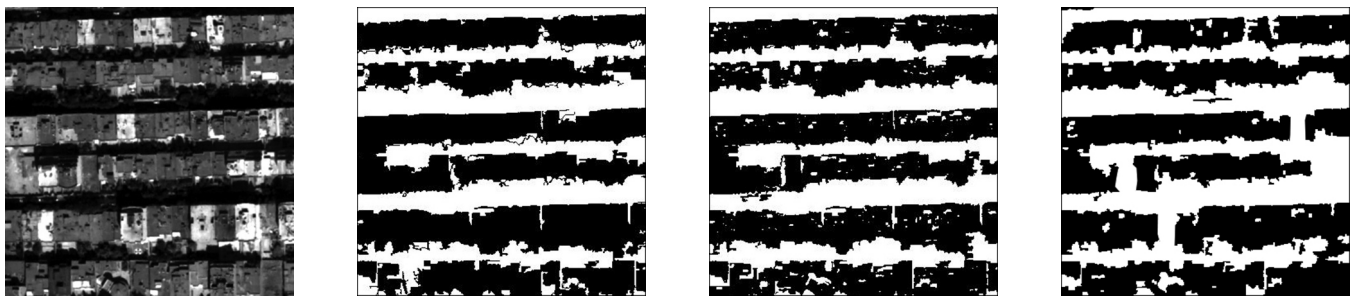

Figure 10. The detection rate of pixel-based algorithms has been more than *OB-ES* algorithm at (a) region (e), (b) *CS* algorithm, (c) *SCM* algorithm, and (d) *OB-ES* algorithm.

Table 3. Accuracy Assessment Results of *OB-ES* Algorithm (%)

Region	DR	R	FNR	FPR	OA
Region (a)	87.05	73.96	12.95	31.76	77.81
Region (b)	95.17	96.32	4.83	24.28	84.50
Region (c)	87.34	88.76	12.66	3.17	94.71
Region (d)	80.18	67.32	19.82	31.53	81.85
Region (e)	86.24	83.62	13.76	21.44	82.85
Region (f)	92.79	79.16	7.21	23.66	84.43
Region (g)	84.19	77.67	15.81	25.89	79.32
Region (h)	89.00	74.67	11.00	39.29	76.70
Region (i)	76.87	62.82	23.13	29.39	73.06
Region (j)	89.16	89.05	10.84	3.78	94.41
MINIMUM	76.87	62.82	4.83	3.17	73.06
MAXIMUM	95.17	96.32	23.13	39.29	94.71
AVERAGE	86.80	79.34	13.20	23.42	82.96
STD	5.44	10.33	5.44	11.69	7.09

Table 4. Accuracy Assessment Results of OB-MS Algorithm (%)

Region	DR	R	FNR	FPR	OA
Region (a)	89.55	81.37	10.45	21.25	84.25
Region (b)	85.36	88.99	14.64	8.68	88.63
Region (c)	87.11	74.41	12.89	8.60	90.45
Region (d)	89.71	65.33	10.29	33.63	76.03
Region (e)	90.68	83.32	9.32	23.05	84.63
Region (f)	95.25	75.96	4.75	29.20	82.83
Region (g)	82.43	76.00	17.57	27.83	77.47
Region (h)	72.63	87.62	27.37	13.36	78.72
Region (i)	83.74	65.82	16.26	28.09	76.55
Region (j)	81.73	80.13	18.27	6.98	90.13
MINIMUM	72.63	65.33	4.75	6.98	76.03
MAXIMUM	95.25	88.99	27.37	33.63	90.45
AVERAGE	85.82	77.90	14.18	20.07	82.97
STD	6.24	8.08	6.24	9.89	5.59

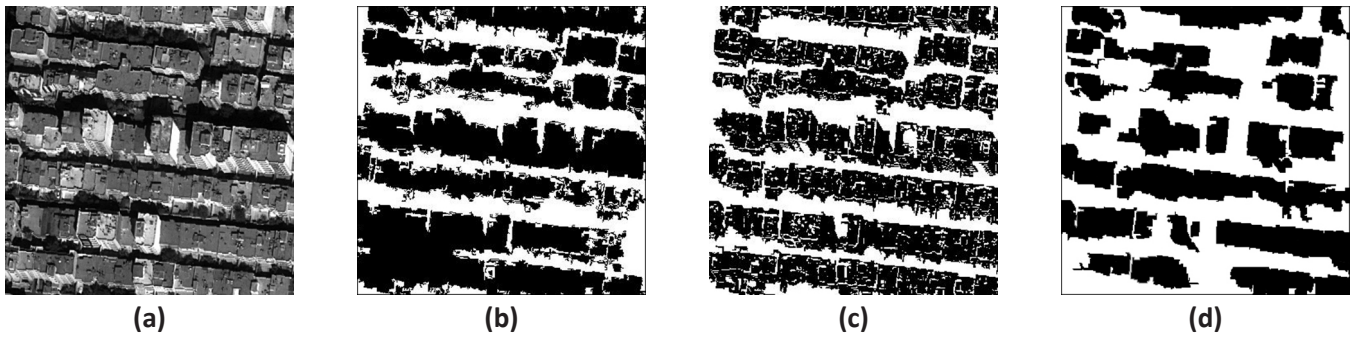

Figure 11. The detection rate of pixel-based algorithms has been more than *OB-MS* algorithm at (a) region (h), (b) *CS* algorithm, (c) *SCM* algorithm, and (d) *OB-MS* algorithm.

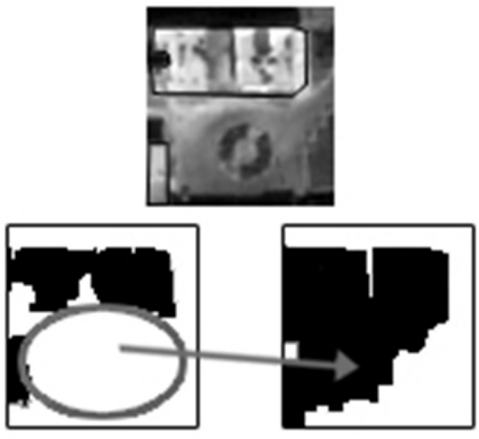

Figure 12. The commission error of *OB-MS* algorithm is more than *SCM* algorithm.

Conclusions

This paper has evaluated and compared four building detection algorithms; two pixel-based and two object-based algorithms using a diverse set of high-resolution satellite imagery. The results indicated that the object-based algorithms were more successful than the pixel-based algorithms in the detection of buildings due to the use of segments or objects instead of single pixels and the non-spectral attributes (i.e., spatial and geometry attributes) in the process. In other words, the performance and the reliability of object-based algorithms were better and higher than pixel-based algorithms. However, the pixel-based methods can produce satisfactory results in some cases. In addition, in some cases, the omission (FNR) and commission (FPR) errors of the object-based algorithms were higher than the pixel-based algorithms. This stems from the segmentation errors in object-based algorithms. In fact, although segmentation is an advantage for the object-based image analysis as compared to the pixel-based analysis, nevertheless it can be a disadvantage for it due to the segmentation errors, i.e., over-segmentation and under-segmentation errors.

References

Aytekin, O., A. Erener, I. Ulusoy, and H.S.B. Duzgun, 2012. Unsupervised building detection in complex urban environments from multispectral satellite imagery, *International Journal of Remote Sensing*, 33(7):2152–2177.

Baatz, M., and A. Schape, 2000. Multiresolution segmentation - An optimization approach for high quality multi-scale image segmentation, *Angewandte Geographische Informations verarbeitung XII* (J. Strobl and G. Griesebner, editors), AGIT Symposium, Salzburg, Germany, pp. 12–23.

Benz, U.C., P. Hofmann, G. Willhauck, I. Lingenfelder, and M. Heynen, 2004. Multi-resolution, object-oriented fuzzy analysis of remote sensing data for GIS-ready information, *ISPRS Journal of Photogrammetry and Remote Sensing*, 58(2004):239–258.

Blaschke, T., 2010. Object-based image analysis for remote sensing, *ISPRS Journal of Photogrammetry and Remote Sensing*, 65(1):2–16.

Bouziani, M., K. Goita, and D.-C. He, 2010. Rule-based classification of a very high resolution image in an urban environment using multispectral segmentation guided by cartographic data, *IEEE Transactions on Geoscience and Remote Sensing*, 48(8):3198–3211.

Cleve, C., M. Kelly, F.R. Kearns, and M. Moritz, 2008. Classification of the wildland-urban interface: A comparison of pixel- and object-based classifications using high-resolution aerial photography, *Computers, Environment and Urban Systems*, 32(2008):317–326.

Ghanea, M., P. Moallem, and M. Momeni, 2011. Automatic extraction of building in a dense urban area from very high resolution satellite images, *Proceedings of the 5th Symposium in Advances in Science and Technology, Mashhad, Iran*, May 2011.

Chubey, M.S., S.E. Franklin, and M.A. Wulder, 2006. Object-based analysis of Ikonos-2 imagery for extraction of forest inventory parameters, *Photogrammetric Engineering & Remote Sensing*, 72(4):383–394.

Hai-yue, L., W. Hong-qi, and D. Chi-biao, 2006. A new solution of automatic building extraction in remote sensing images, *IEEE International Conference on Geoscience and Remote Sensing Symposium, 2006*, IGARSS 2006, pp. 3790–3793.

Hester, D.B., H.I. Cakir, S.A.C. Nelson, and S. Khorram, 2008. Per-pixel classification of high spatial resolution satellite imagery for urban land-cover mapping, *Photogrammetric Engineering & Remote Sensing*, 74(4):463–471.

Holbling, D., and M. Neubert, 2008. ENVI Feature Extraction 4.5, Snapshot, *GIS Business*, pp. 48–51.

Hu, X., and Q. Weng, 2011. Impervious surface area extraction from IKONOS imagery using an object-based fuzzy method, *Geocarto International*, 26(1):3–20.

Huang, X., and L. Zhang, 2011. A multidirectional and multiscale morphological index for automatic building extraction from multispectral GeoEye-1 imagery, *Photogrammetric Engineering & Remote Sensing*, 77(7):721–732.

Huang, X., and L. Zhang, 2012. Morphological building/shadow index for building extraction from high-resolution imagery over urban areas, *IEEE Journal of Selected Topics in Applied Earth Observations and Remote Sensing*, 5(1):161–172.

Huang, X., and L. Zhang, 2013. An SVM ensemble approach combining spectral, structural and semantic features for the classification of high resolution remotely sensed imagery, *IEEE Transactions on Geoscience and Remote Sensing*, 51(1):257–272.

Jiang, N., J.X. Zhang, H.T. Li, and X.G. Lin, 2008. Semi-automatic building extraction from high resolution imagery based on segmentation, *International Workshop on Earth Observation and Remote Sensing Applications, 2008*, EORSA 2008, pp. 1–5.

Jin, X., and C.H. Davis, 2005. Automated building extraction from high-resolution satellite imagery in urban areas using structural, contextual and spectral information, *EURASIP Journal on Applied Signal Processing*, 14:2196–2206.

Kanjir, U., T. Veljanovski, A. Marsetic, and K. Ostir, 2008. Application of object-based approach to heterogeneous land-cover/use, *The International Archives of the Photogrammetry, Remote Sensing and Spatial Informational Sciences*, XXXVIII-4/C7.

Khoshelham, K., C. Nardinocchi, E. Frontoni, A. Mancini, and P. Zingaretti, 2010. Performance evaluation of automated approaches to building detection in multi-source aerial data, *ISPRS Journal of Photogrammetry and Remote Sensing*, 65:123–133.

Lee, D.S., J. Shan, and J.S. Bethel, 2003. Class-guided building extraction from Ikonos imagery, *Photogrammetric Engineering & Remote Sensing*, 69(2):143–150.

Meng, X., L. Wang, and N. Currit, 2009. Morphology-based building detection from airborne lidar data, *Photogrammetric Engineering & Remote Sensing*, 75(4):427–442.

Meng, X., N. Currit, L. Wang, and X. Yang, 2012. Detect residential buildings from lidar and aerial photographs through object-oriented land-use classification, *Photogrammetric Engineering & Remote Sensing*, 78(1):35–44.

Mura, M.D., J.A. Benediktsson, B. Waske, and L. Bruzzone, 2010. Morphological attribute profiles for the analysis of very high-resolution images, *IEEE Transactions on Geoscience and Remote Sensing*, 48(10):3747–3762.

Myint, S.W., P. Gober, A. Brazel, S. Grossman-Clarke, and Q. Weng, 2011. Per-pixel vs. object-based classification of urban land cover extraction using high spatial resolution imagery, *Remote Sensing Environment*, 115(5):1145–1161.

Taubenbuck, H., T. Esch, M. Wurm, A. Roth, and S. Dech, 2010. Object-based feature extraction using high spatial resolution satellite data of urban area, *Journal of Spatial Science*, 55(1):117–132.

Wang, P., X. Feng, S. Zhao, P. Xiao, and C. Xu, 2007. Comparison of object-oriented with pixel-based classification techniques on urban classification using TM and IKONOS imagery, *Proceedings of SPIE*, Vol. 6752, 67522J.

Wei, Y., Z. Zhao, and J. Song, 2004. Urban building extraction from high-resolution satellite panchromatic image using clustering and edge detection, *Proceedings of IGARSS '04, IEEE International Geoscience and Remote Sensing Symposium*, 3:2008–2010.

(Received 18 June 2013; accepted 14 January 2014; final version 27 January 2014)